

We are IntechOpen, the world's leading publisher of Open Access books Built by scientists, for scientists

5,600

Open access books available

137,000

International authors and editors

170M

Downloads

Our authors are among the

154

Countries delivered to

TOP 1%

most cited scientists

12.2%

Contributors from top 500 universities



WEB OF SCIENCE™

Selection of our books indexed in the Book Citation Index
in Web of Science™ Core Collection (BKCI)

Interested in publishing with us?
Contact book.department@intechopen.com

Numbers displayed above are based on latest data collected.
For more information visit www.intechopen.com



Silk Fibroin Nanoparticles: Synthesis and Applications as Drug Nanocarriers

Guzmán Carissimi, Mercedes G. Montalbán, Marta G. Fuster and Gloria Villora

Abstract

The use of nanoparticles in biomedical fields is a very promising scientific area and has aroused the interest of researchers in the search for new biodegradable, biocompatible and non-toxic materials. This chapter is based on the features of the biopolymer silk fibroin and its applications in nanomedicine. Silk fibroin, obtained from the *Bombyx mori* silkworm, is a natural polymeric biomaterial whose main features are its amphiphilic chemistry, biocompatibility, biodegradability, excellent mechanical properties in various material formats, and processing flexibility. All of these properties make silk fibroin a useful candidate to act as nanocarrier. In this chapter, the structure of silk fibroin, its biocompatibility and degradability are reviewed. In addition, an intensive review on the silk fibroin nanoparticle synthesis methods is also presented. Finally, the application of the silk fibroin nanoparticles for drug delivery acting as nanocarriers is detailed.

Keywords: silk fibroin, structure, biocompatibility, nanoparticle, synthesis, nanocarrier

1. Introduction

Silk is an ancestral material used since 2450 BC [1] for making fabrics. After having been an economic engine of several empires and coining the name to the trade route that linked Asia, Europe and Africa, silk suffered a debacle in the early 20th century when the much cheaper synthetic polymers derived from hydrocarbons were introduced. However, today, motivated by its biocompatibility and excellent mechanical properties, researchers around the world are trying to produce biomaterials based on this biopolymer for a variety of biomedical applications: films with a surface roughness that increase cell adhesion, 3D structures for bone implants, hydrogels for wound protection and nanoparticles for drug delivery, among others [2–5].

Silk fibroin probably receives a lot of attention from the general public due to its mechanical properties, so a brief text will be devoted to comparing them with other natural fibers and engineering materials. **Table 1** shows values of stress at break, elasticity and percentage of nominal deformation at the break of silk fibroin together with the values of other biomaterials and synthetic materials. Excluding

Material	Tension at break (MPa)	Elasticity (GPa)	% nominal strain at break	Ref.
Silk <i>B. Mori</i> (with sericin)	500	5–12	19	[6]
Silk fibroin <i>B. mori</i>	610–690	15–17	4–16	[6]
Spider silk <i>N. clavipes</i>	875–972	11–13	17–18	[7]
Collagen ^a	0.9–7.4	0.0018–0.046	24–68	[8]
Collagen ^b	42–72	0.4–0.8	12–16	[8]
PLA ^c	28–50	1.2–3.0	2–6	[9]
Tendon (mostly collagen)	150	1.5	12	[10]
Bone	160	20	3	[10]
Kevlar (49 fibers)	3600	130	2.7	[10]
Carbon fiber	4000	300	1.3	[10]
Synthetic rubber	50	0.001	850	[10]

^aType I collagen fibers extruded from rat tail tested after stretching from 0–50%.
^bCross-linked rat tail collagen tested after stretching from 0–50%.
^cPoly(lactic acid) with molecular weights ranging from 50,000 to 300,000 units.
Adapted from reference (5) with permission of Elsevier.

Table 1.

Comparison of the mechanical properties of different natural and synthetic fibers.

mineralized biomaterials (bones), Kevlar and carbon fibers, *Bombyx mori* silk fibroin together with *Nephila clavipes* spider silk are the biomaterials with the highest stress at break. While the list of biomaterials is incomplete, it is fair to say that fibroins are among the strongest polymeric biomaterials known. However, the tensile strength of fibroin is substantially lower than that of Kevlar and carbon fiber, engineering materials that are commonly used to transmit and support tensile forces. At first glance, we could infer that fibroin is superior to other biomaterials, such as collagen, but not as “good” as Kevlar and carbon fibers. However, this interpretation is based on the assumption that “good” means stiff and strong. Looking closely at **Table 1**, it can be seen that fibroin is quite extensible, presenting a maximum deformation of approximately 18%, while engineering materials fail in deformations of the order of 1–3%. The great extensibility of fibroin makes it more resistant than engineering materials.

It is especially notable that silkworms can produce strong and stiff fibers at room temperature and from an aqueous solution, while synthetic materials with comparable properties must be processed at elevated high temperatures and/or with less benign solvents. Furthermore, synthetic polymer fibers typically require post-spin stretching to ensure the necessary degree of molecular orientation in their structure [11]. On the other hand, this is not necessary for silk in the natural spinning process. This is due to its impressive amino acid sequence which gives rise to an extraordinary polymorphic secondary structure that will be discussed below.

2. Silk structure

Silk is a protein biopolymer synthesized by a wide variety of lepidoptera and arachnids in specialized glands. However, it is important to note that this chapter focuses on silk fibroin from the silkworm *Bombyx mori* of the *Bombycidae* family, fed only with mulberry leaves (*Morus alba* L.). This is important because the amino acid sequence

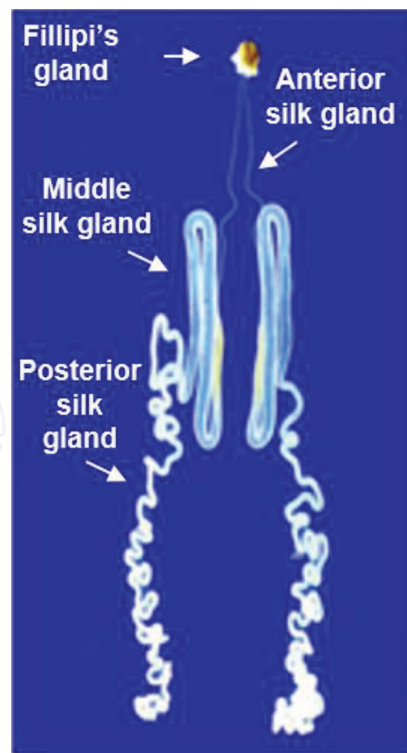


Figure 1.
Diagram of the silk fibroin gland. From reference [12] with permission of public library of science (PLOS).

varies from species to species and with it its mechanical and physicochemical properties, which can have great implications in different applications.

Silk proteins are synthesized in a gland that extends through the abdomen of the worm and is divided into three sections, posterior, middle and anterior, as illustrated in **Figure 1**. The posterior gland cells secrete silk fibroin, reaching a concentration of approximately 12% by weight. At this time, the protein is in a water-soluble state [13], with a partially ordered secondary structure composed of irregular structures and type II β -turns [14], commonly known as *silk I*. This protein is pushed into the gland media, where cells lining the lumen secrete sericin along with other flavonoids (assimilated by worms in the diet) [15]. Fibroin and sericin are concentrated to 25% by weight and are driven to the anterior gland where they experience pH gradients (maintained through the secretion of carbonic anhydrase) and ionic strength gradients. These factors contribute to the elongation of fibroin (at this point 30% by weight) into two thin filaments and promote the crystallization of repetitive domains. Lastly, during the spinning process, the non-Newtonian protein solution is subjected to crystallization induced by changes in pH and ionic strength through the gland [16] and by the shear stress generated by an opposing pressure front to the flow, generating a velocity gradient from the inlet (0.334 mm/s) to the outlet (13.8 mm/s) of the spinning organ [17]. Throughout the process, the silk fibroin initially secreted with a partially ordered structure (*silk I*) undergoes a transition to one composed mainly (58%) [18] by antiparallel β sheets, adopting an insoluble crystalline structure known as *silk II* [18, 19].

To understand the formidable properties of this biopolymer, its structure must be studied in detail. A silk cocoon is composed of a single silk fiber between 1000 and 1500 m in length with a diameter of between 10 and 25 μm [20]. This fiber is composed of a core of two fibroin filaments, each one of approximately 10 μm covered by a layer of sericin that hold the fibers together, as illustrated in **Figure 2** left, providing greater resistance to the assembly of the fiber. In turn, fibroin fibers are

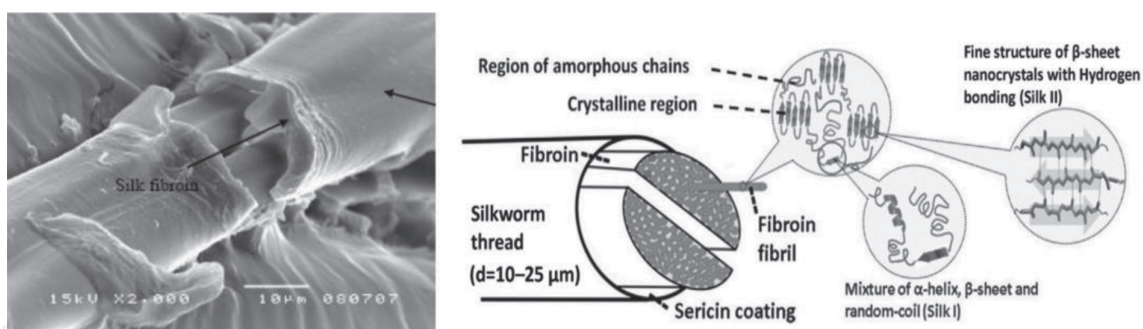


Figure 2.

Left, scanning electron microscope image (2,000X magnification) of silk fiber, containing two fibroin fibers coated by sericin. From reference [21] with permission of Elsevier. Right, schematic representation of the structure of silk fibroin. Insets show the general structure of the fibrils and the alignment of the antiparallel β-sheets. From reference [22] with permission of John Wiley and Sons.

composed of coiled nanofibrils of between 20 and 25 nm, which gives them greater tensile strength (Figure 2, right) [23].

Fibroin, representing approximately 75% of the weight of the cocoon, is a linear, water-insoluble protein with high tensile strength. On the other hand, sericin represents approximately 25% of the cocoon weight, it is a globular, water-soluble protein whose function is to keep the fibroin fibers together [24]. Silk fibroin is made up of three components, a heavy chain (391 kDa) and a light chain (26 kDa) linked by a disulfide bridge, and a glycoprotein, P25 (25–30 kDa) in a 6: 6: 1 molar ratio to yield a 6.3 MDa megastructure [25]. The primary structure of the silk fibroin heavy chain is schematically represented in Figure 3A. This chain is composed of 5,263 amino acids divided into N- and C-terminal domains, both hydrophilic, and

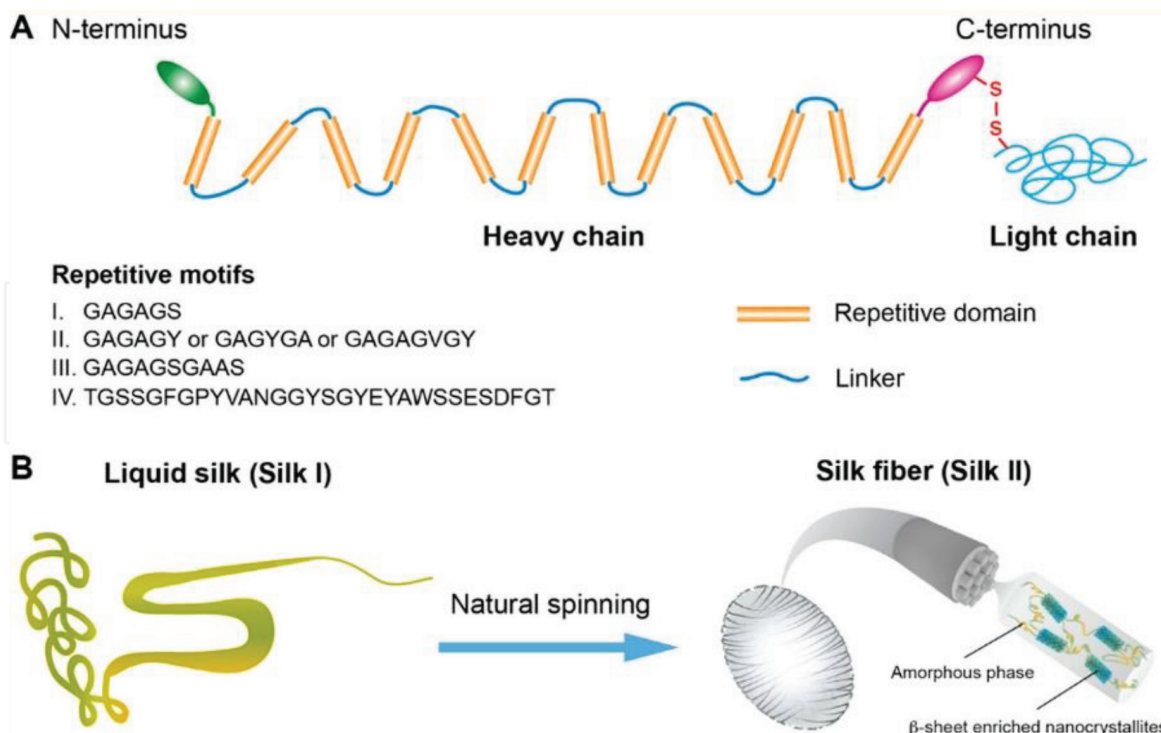


Figure 3.

Organization of the amino acid sequence within silk fibroin. A) In green and magenta, the N- and C-terminal domains are shown, respectively. The repetitive sequences of the GAGAGS type that give rise to the crystalline domains of the silk fibroin are represented by orange cylinders and in blue, the hydrophilic sequences that flank the crystalline regions. B) Diagram representing the transition from water-soluble silk (silk I) to crystalline silk fibers after the bio-spinning process. In silk fiber, amorphous regions (44%) and crystalline regions rich in antiparallel β sheets (56%) are represented. Reprinted with permission from reference [26]. Copyright 2020 American Chemical Society.

12 hydrophobic domains flanked by 11 short and hydrophilic domains. The hydrophobic domains contain highly conserved and repetitive sequences of the GAGAGS, GAGAGY, and GAGAGVGY types that form the β -sheet structures that, in addition, are packaged in crystalline areas [16]. 86% of the amino acids of the heavy chain of fibroin are Glycine (45%), Alanine (29%) and Serine (12%) [27], which are mostly found in the hydrophobic and highly repetitive regions. The great bias that the primary sequence of fibroin presents towards amino acids with small residues such as Glycine and Alanine, promotes the formation of antiparallel β -sheets, which are mostly packed in the crystalline areas.

The secondary structure of fibroin contains approximately a total of 58% of β -sheet [28], of which approximately 33% correspond to antiparallel β -sheets organized in crystalline structures. Fibroin fibers are generally described as a matrix of disordered structures with β -sheet crystals embedded in it [26], as represented in **Figure 3B**. The intra and intermolecular hydrogen bond network provide strength and tensile strength to the biopolymer, while amorphous regions provide flexibility and elasticity [29]. In the literature, there is great variability in the sizes reported for these crystals [30–33]. To illustrate the size of these, reference can be made to X-ray diffraction measurements and low voltage transmission electron microscopy performed by Drummy et al. [30]. They have determined that the crystals within the fibroin fibers have dimensions of 21 x 6 x 2 nm and their major axis is aligned parallel to the axis of the fibers.

The secondary structure of fibroin with *silk II* conformation is extremely stable thanks to a large number of hydrogen bonds which makes it insoluble in most solvents, including under moderate acidic and alkaline conditions. As the content of acidic and basic groups is low in fibroin, the electrostatic factor is not decisive in the formation of the secondary structure, however, it can be decisive in the dissolution of fibroin. The secondary structure of fibroin is not only relevant in the biomaterial synthesis process due to the need for its dissolution, but also due to its influence on the mechanical and physicochemical properties of the resulting biomaterials. For example, Wang et al. [34] prepared silk and polyvinylpyrrolidone micro- and silk fibroin nanoparticles for controlled drug release and concluded that release profiles can be adjusted by modulating the number of β -sheets in the secondary structure of fibroin.

3. Silk biocompatibility

Silk fibroin is an attractive material for numerous biomedical applications as, due to its mechanical and physicochemical properties, it encompasses applications such as drug delivery, tissue engineering, and implantable devices. However, in addition to the functionalities necessary for specific applications, a key factor necessary for the clinical success of any biomaterial is the appropriate in vivo interactions with the body or biocompatibility. Among them, (i) the immune and inflammatory response and (ii) the biodegradability can be studied.

3.1 Immune and inflammatory response

As already mentioned, silk fiber is essentially made up of two proteins, fibroin and sericin. While fibroin is highly biocompatible [3, 4] with a low immune response [35, 36], sericin can present unwanted adverse allergic reactions [37, 38]. For this reason, sericin is normally removed by different procedures, known as degumming [39]. Depending on the format of the material and the location of implantation, silk fibroin can induce a mild inflammatory response that diminishes within a few hours/days after implantation [40]. The response involves the recruitment and

activation of macrophages and may include the activation of a mild foreign body response with the formation of multinucleated giant cells, again depending on the format of the material and the location of implantation [36]. The number of immune cells decreases with time, and granular tissue, if formed, is replaced by endogenous non-fibrous tissue, although these responses are reserved for films, hydrogels, and bone implants [36].

The study carried by Meinel et al. [40] indicated that collagen films implanted in rats produce a greater inflammatory reaction in the tissue than equivalent films prepared with fibroin after 6 weeks. In another study comparing fibroin membranes and poly (styrene) and poly (2-hydroxyethyl methacrylate) membranes, Santin et al. [41] demonstrated that the former has a milder immune response than the latter. The results indicated that lower levels of fibrinogen were bound to the fibroin membrane than to the two synthetic polymers, while the same amounts of C₃ human plasma complement fragment and adsorbed IgG were detected. The activation of mononuclear cells by fibroin, measured as production of interleukin 1 β , was lower than that of synthetic materials. Another study indicated that the braided silk fibroin used for the reconstruction of the anterior cruciate ligament produces a mild inflammatory response after seven days of implantation in vivo, while an equivalent implant made with the biodegradable polymer polyglycolic acid (PGA) produced a more acute response [42]. In this case, although the breaking load for the PGA implant was twice that for the fibroin graft, the initial attachment and growth of cells in the prosthetic ligament was higher in the latter.

In the case of silk fibroin nanoparticles, the literature is not as extensive as for other formats of the same material. Tan et al. [43] showed that nanoparticles coated with fibroin hardly produced an immune response and the adaptive immune system was not activated. In another study, Totten et al. [44] used in vitro and nuclear magnetic resonance-based metabolomics assays to examine the inflammatory phenotype and metabolic profiles of macrophages after exposure to PEGylated and unmodified silk fibroin nanoparticles. The macrophages internalized both types of nanoparticles but showed different phenotypic and metabolic responses to each type of nanoparticle. Unmodified silk fibroin nanoparticles induced upregulation of several processes, including the production of pro-inflammatory mediators (such as cytokines), the release of nitric oxide, and the promotion of antioxidant activity. These responses were accompanied by changes in macrophage metabolomic profiles that were consistent with a pro-inflammatory state and indicated an increase in glycolysis and reprogramming of the tricarboxylic acid cycle and the creatine kinase/phosphocreatine pathway. In contrast, PEGylated silk fibroin nanoparticles induced milder changes in inflammatory and metabolic profiles, suggesting that immunomodulation of macrophages with silk fibroin nanoparticles is dependent on PEGylation. This would indicate that the PEGylation of silk fibroin nanoparticles reduces the inflammatory and metabolic responses initiated by macrophages. In the case of silk fibroin microparticles (10–200 μ m) prepared by enzymatic digestion, Panilaitis et al. [38] found that suspension of the particles induced a significant release of TNF cytokines. In contrast, macrophages grown in the presence of silk fibroin fibers did not upregulate transcription levels for a wide range of pro-inflammatory cytokines to a significant degree. The combination of results from these two studies could indicate that the immune response is dependent on the size of the biomaterial, excluding materials at the nanoscale and macroscale, but not at the microscale. In a recent study carried out in our research group [45], the HeLa and EA.hy926 cell lines were incubated with up to 250 μ g/mL of silk fibroin nanoparticles in vitro. Viability was studied by MTT tests, and the results did not show significant variations ($p < 0.05$) with respect to the controls.

Recent studies indicated that nanoparticles loaded with resveratrol have shown immunomodulatory properties and anti-inflammatory effects in murine models with inflammatory bowel disease [46] and periodontal infections [47]. In another similar study [48], treatments with RGD linear peptide-functionalized silk fibroin nanoparticles were performed and were found to improve colonic damage in rats, reduce neutrophil infiltration, and improve the compromised oxidative state of the colon. It was also found that only rats treated with RGD-silk fibroin nanoparticles showed a significant reduction in the expression of different pro-inflammatory cytokines (interleukin-1 β , IL-6 and IL-12) and inducible nitric oxide synthase compared to the control group. Furthermore, the expression of both cytokine-induced neutrophil chemoattractant-1 and monocyte chemoattractant protein-1 was significantly decreased with RGD-silk fibroin nanoparticle treatment.

3.2 In vivo degradation of silk fibroin

Fibroin fibers implanted in the human body retain more than 50% of their mechanical properties after 60 days, which is why the North American Pharmacopeia classifies this material as non-biodegradable [49]. However, the rate at which fibroin degrades depends on the size of the implanted material, its morphology, mechanical and biological conditions at the implantation site, the secondary structure of the protein, and the molecular weight distribution of the fibroin chains. In particular, for the application of silk fibroin nanoparticles to drug transport, three of these parameters must be taken into account mainly: (i) size, (ii) molecular weight distribution and (iii) secondary structure. But before analyzing each of them, the possible degradation pathways of fibroin will be discussed to later mention how these parameters are able to influence degradation.

As a protein, fibroin exhibits degradation against proteases capable of degrading amide bonds including α -chymotrypsin, collagenase IA, protease XIV, and metalloproteases [50–52]. The residues of the degradation process are the corresponding amino acids of the proteins, so they are easily absorbed in vivo and do not generate toxicity. The partial hydrolysis of the protein by enzymes into small fragments is not a problem either, since these can be easily phagocytosed by macrophages [38]. Li et al. [51] observed that the mean molecular weight of fibroin film products after degradation with the three enzymes followed the order of protease XIV > collagenase IA > α -chymotrypsin. The degradation mechanism is based on a two-stage process, based on enzymes finding binding domains on the surface of materials and their subsequent hydrolysis [53]. In this manner, different enzymes have different results for the degradation of different structures within fibroin. For example, chymotrypsin has been used to degrade the amorphous regions of fibroin to obtain highly crystallized fibroin [51]. Collagenase preferentially degrades the content of β sheets in hydrogels [38]. On the other hand, after incubation of fibroin with protease XIV, it was found that the mass was significantly reduced [51]. Brown et al. [38] concluded that the ability of enzymes to break down a biomaterial not only depends on the cleavage sites being present in the primary structure of the protein but also the secondary structure and the format of the material play a fundamental role. This indicates that the degradability of fibroin can be modulated by controlling the relative abundance of its secondary structures. In this way, for example, by reducing the content of highly crystalline structures in stacked β -sheets, degradation can be accelerated, since both protease XIV and chymotrypsin can act simultaneously in these areas.

Horan et al. [49] concluded that the degradation of electrospun fibers exhibited a predictable degradation dependent on the diameter of the fibers. As expected, as the diameter decreases and, therefore, the surface/volume ratio increases, the

degradation occurs at a higher rate. Decreasing the size from macroscopic fibers to nanoparticles will clearly increase this ratio, allowing greater access to enzymatic degradation and phagocytosis by macrophages. The degradation of PEG-functionalized and non-functionalized silk fibroin nanoparticles by proteolytic enzymes (protease XIV and α -chymotrypsin) and papain, as well as cysteine protease, were studied by Wongpinyochit et al. [54]. Both classes of particles presented similar degradation patterns in a period of 20 days, establishing the order of degradation of the particles by means of enzymes such as: Protease XIV > papain > α -chymotrypsin. The authors reported that, after 1 day, silk fibroin nanoparticles and PEG-silk fibroin nanoparticles incubated with protease XIV lost 60 and 40% of their mass, respectively, a reduction in the amorphous content of the secondary structure and an increase in diameter. In contrast, 10 days of incubation were required for similar degradations with papain and 20 with α -chymotrypsin. Silk fibroin nanoparticles were also exposed to a complex mixture of rat liver lysosomal enzymes *ex vivo*, finding that they lost 45% of their mass in 5 days.

Lastly, it should be noted that modifications in the molecular weight distribution of fibroin chains can alter the rate of degradation [55]. A decrease in this can alter the order of crosslinking between polymers and potentially result in faster degradation [56]. For this reason, the purification and subsequent processing of fibroin not only affects the mechanical and physicochemical properties of the resulting biomaterials [57] but can also be used to modulate their biodegradability.

4. Synthesis of silk fibroin nanoparticles

Silk fibroin particles can be produced from the top-down as well as the bottom-up approach. The first of these involves grinding the fibroin fibers to reduce their size. This can be achieved through ball milling [58, 59], bead milling [60], air-jet [61] as well as irradiating the material with an electron beam [62]. However, these tend to produce particles in the micrometer range and with a wide size distribution, so in the rest of this section, we will focus on the bottom-up approach which offers more control over the particles produced. This approach is based on the self-assembly of the smallest units that constitute a nanoparticle. In the particular case of silk fibroin nanoparticles, the fibroin fibers are firstly dissolved to obtain their individual constituent units and subsequently regenerated into nanoparticle format. This is normally achieved through a desolvation process, which can be achieved in different ways that will be discussed in this section along with some examples; but first, the dissolution of silk fibroin will be discussed, which is not an easy task due to its high structural stability and deserves a detailed analysis that will be exposed below.

4.1 Solubilization of silk fibroin

The preparation of most biomaterials depends on achieving a complete dissolution of fibroin. This process is referred to by some authors as reverse engineering [63], since it attempts to obtain water-soluble fibroin with *silk I* structure, starting from fibers with *silk II* structure. However, only a limited number of solvents are able to dissolve silk fibroin. Examples of these are strong acidic solutions (phosphoric, formic, sulfuric, hydrochloric) or aqueous/organic solutions concentrated in salts (LiCNS, LiBr, CaCl₂, Ca (CNS)₂, ZnCl₂, NH₄CNS, CuSO₄, NH₄OH, Ca(NO₃)₂) those that are capable of completing the dissolution of fibroin fibers [64–70]. This is due to the presence of the great network of intra- and intermolecular hydrogen bonds and the high crystallinity derived from its secondary structure.

In general, the literature describes the dissolution of fibroin in concentrated salt solutions as a two-step process [64, 67]. In the first step, the compact, crystalline structure of fibroin fibers swells due to the diffusion of solvent molecules. In the second, the dispersion of the silk fibroin molecules begins due to the collapse of the intermolecular interaction and their consequent dissolution [67]. During dissolution, amorphous sections with a higher content of massive amino acid residues or polar groups are firstly dissolved. The cations (Ca^{2+} , Zn^{2+} , Cu^{2+} , NH_4^+ , Li^+) form stable chelate complexes with hydroxyl groups of the serine and tyrosine side chains and also with the oxygen of the carbonyls, breaking the hydrogen bonds and the van der Waals forces between polypeptide chains resulting in the dissolution of the protein that adopts *silk I* structure [68, 70, 71].

The described dissolution process depends on reaching a high concentration of salts. This entails certain disadvantages since extensive dialysis (72 h) is required to eliminate these, which requires 6 liters of distilled water for every 12 mL of solution [64]. Furthermore, the solutions obtained are unstable and tend to gel within a period of days. Alternatively, when long-term storage of fibroin is desired, aqueous fibroin solutions can be lyophilized and subsequently dissolved in organic solvents such as hexafluoroisopropanol [64] at the time they are to be used. However, these solvents are toxic and extremely corrosive so they require special care when handling [72].

Recently, ionic liquids have emerged as an alternative for the dissolution of silk fibroin [73] providing numerous advantages over traditional methods [64, 65]. Firstly, the negligible vapor pressure and easy recyclability of ionic liquids make them a more “green” alternative to organic solvents [74–76]. Secondly, the possibility of obtaining high concentrations of fibroin in a stable solution (up to 25% w/w in some ionic liquids [77]). Fibroin solutions in ionic liquids are more stable because the hydrophobic regions (highly conserved GAGAGS or GAGAGAGS sequences) are stabilized by the alkyl chains of cations such as imidazolium [78]. On the other hand, the bulky charged imidazolium ring is oriented outwards providing electrostatic repulsive forces between the hydrophobic blocks and preventing the transition from *silk I* to *silk II* through the formation of the β sheets. According to Wang et al. [78], solutions of silk fibroin in 1-allyl-3-methylimidazolium chloride can be stable for periods longer than one and a half years. Thirdly, the ease with which silk fibroin can be dissolved. According to the method described by Lozano-Pérez et al. [77], by means of high-power ultrasound, the complete dissolution of fibroin can be achieved in a few minutes compared to several hours with traditional methods [64, 65].

4.2 Regeneration of fibroin into nanoparticles

Nanoparticle synthesis processes in a bottom-up approach involve the dissolution of fibroin in its constituent polymer units and its subsequent regeneration into nanoparticles. This regeneration is normally carried out by means of a desolvation process in an “antisolvent”, a process commonly referred to as antisolvation. As shown in **Figure 4**, in the nanoparticle synthesis process by antisolvation there are three key components, the polymer, the solvent and the antisolvent. The necessary conditions are that: (i) the solvent and the antisolvent are miscible under the process conditions, while (ii) the solute must be insoluble in the solvent/antisolvent mixture. In this way, when mixing the polymer solution, the antisolvent will seize the molecules that solvate it, leading to their aggregation. Employing kinetic and thermodynamic controls, a limited number of polymer units can be made to aggregate, thus forming nanoparticles. In practice, the preparation of nanoparticles by antisolvation can be achieved by different techniques that vary in the methodology

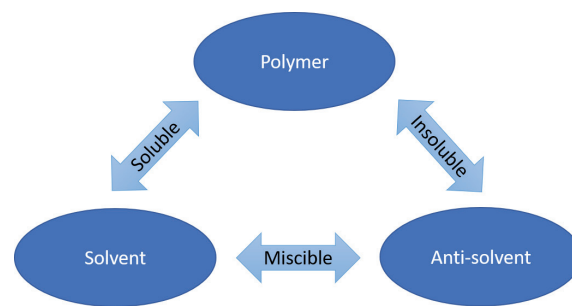


Figure 4.
Key components in the antisolvation process.

of mixing the solution of the polymer and the antisolvent or the nature of the latter. We will describe some of the most representative methods in the literature below.

4.2.1 Antisolvation in organic solvents

Probably one of the most widely used methods due to its simplicity and good results is the addition of the silk fibroin solution to water-miscible polar organic solvents, which act as an antisolvent when initiating the transition from *silk I* to *silk II* through the β -sheet formation [44, 77, 79–83]. It should be noted that the inverse variant, where the antisolvent is added to the fibroin solution, is also frequently found in the literature [84–86].

As an example, Wongpinyochit et al. [83] dissolved the fibroin fibers in a 9.3 M LiBr solution, keeping them stirred for 4 hours at 60°C. Subsequently, the solution is dialyzed for 72 hours and centrifuged to remove insoluble residues. Then, the fibroin concentration is adjusted to 5% w/v and added dropwise (10 μ l/drop at a speed of 50 drops/min) to acetone under strong agitation, the volume of acetone being greater than 75% of the final volume of both liquids. A white suspension is immediately formed upon contact of both liquids, marking the formation of the nanoparticles. The particles are washed and collected by centrifugation. The overall process is illustrated in **Figure 5**. An average diameter of ca. 100 nm and a Z-potential of -50 mV (in distilled water) are provided for the particles obtained.

One way to optimize the nanoparticle synthesis process is to reduce the mixing time between the fibroin solution and the antisolvent [87]. This can be achieved by reducing the size of the fibroin solution droplets (increased surface/volume ratio) that come into contact with the antisolvent, favoring mass transfer [87]. In our research group, a method has been developed that uses a coaxial injector where the fibroin solution flows through the center and nitrogen under pressure runs through the concentric cylinder, this manages to produce an aerosol with very small droplets [45, 88].

4.2.2 Antisolvation in supercritical fluids

A supercritical fluid is any substance that is under conditions of pressure and temperature above its critical point. Under these conditions, the substance has hybrid properties between a liquid and a gas, that is, it can diffuse like a gas, and dissolve substances like a liquid [89]. Assuming that the compound to be used as a supercritical fluid meets the conditions described at the beginning of this section, it can act as an antisolvent in an antisolvation process. In this case, the process is known as supercritical antisolvation (SAS). In particular, carbon dioxide (CO₂) is one, if not the most used substance as a supercritical fluid due to its moderate critical conditions (T = 304 K and P = 7.38 MPa), harmless to the operator and the environment, as well as its economic obtaining and operation [89].

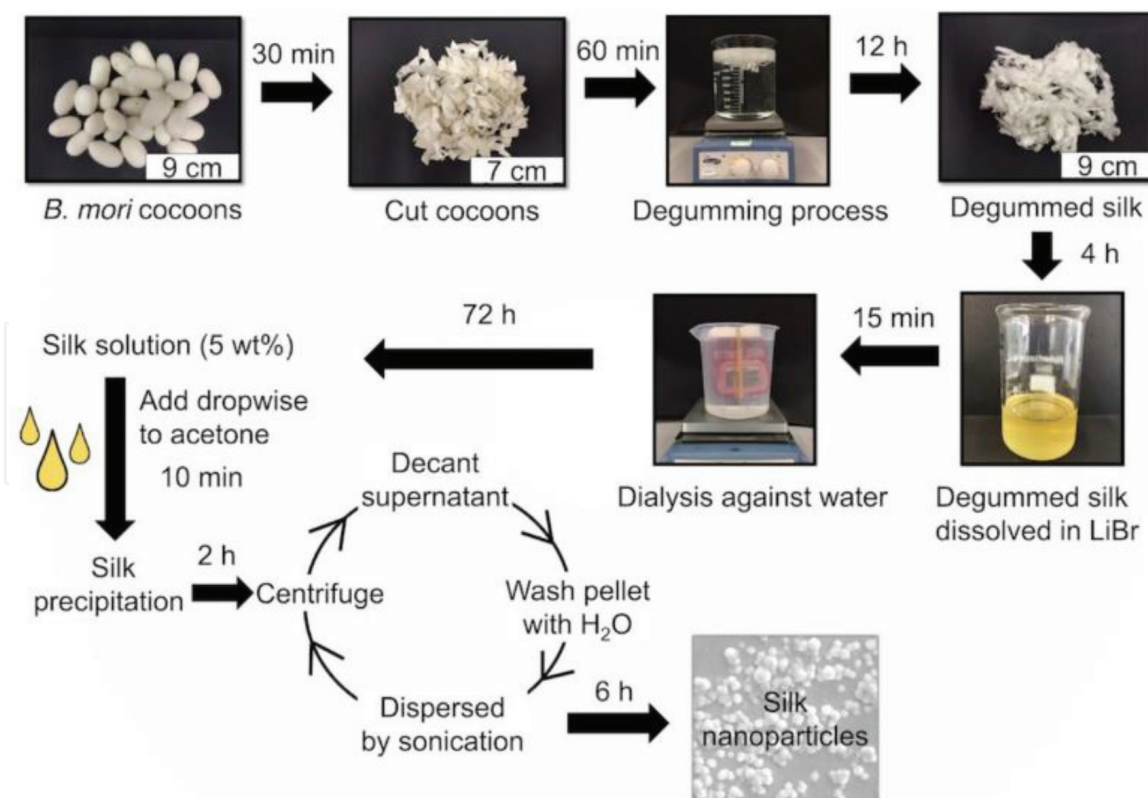


Figure 5. Scheme illustrating the key steps to generate a solution and obtain silk fibroin nanoparticles described by Wongpinoyochit et al. [83]. Reprinted with permission from reference (83). Copyright 2016 MyJoVE corporation.

The SAS process is well known and has been used for the preparation of silk fibroin nanoparticles [90–92]. SAS has some variants by other acronyms: Aerosol Solvent Extraction System (ASES), Solution Enhanced Dispersion by Supercritical Fluids (SEDS), Supercritical AntiSolvent with Enhanced Mass transfer (SAS-EM). The main difference between these processes is in the device for injecting the solution and CO₂. In the case of the SAS and ASES processes, the liquid solution is injected into the precipitation reactor through a micrometric nozzle, in the case of the SEDS process, the nozzle is coaxial; whereas, the SAS-EM process uses a baffle surface that vibrates at ultrasonic frequencies to improve the atomization of the solution [93].

This method can be exemplified by the process outlined by Xie et al. [90] for the preparation of curcumin-loaded silk fibroin nanoparticles by SEDS. Briefly, lyophilized silk fibroin in the *silk I* state is dissolved in hexafluoroisopropanol together with curcumin. The solution is subsequently injected into a precipitation reactor containing CO₂ at 20 MPa which will act as an antisolvent for fibroin. After the complete injection of the solution, a constant flow of CO₂ is maintained to remove the hexafluoroisopropanol from the precipitation reactor. Finally, the reactor is depressurized and opened for the collection of the nanoparticles. The process produces nanoparticles with a mean diameter of less than 100 nm.

4.2.3 Electrospray

Electrospray is a technique in which an electrical potential difference is applied between the nozzle of an injector and a manifold, which can contain a liquid that acts as an antisolvent [94]. In this technique, the surface of the liquid emerging from a capillary subjected to electrical stress is deformed into an elongated injector that initially produces a series of micrometer-sized drops. Because the drops are charged, the repulsive forces break each drop into a group of smaller drops in a process called coulombic explosion [94]. Using this technique to spray a silk fibroin solution onto

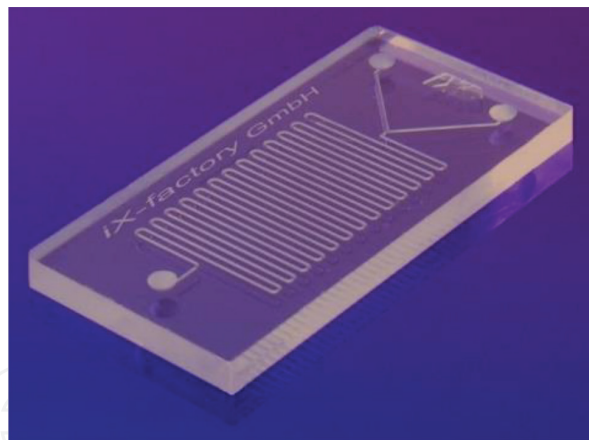


Figure 6. Microfluidic chip made of glass. Channels are 50 μm deep and 150 μm wide (image by IX-factory STK, 2014, CC BY-SA 3.0; no changes were made to the original image).

aluminum foil, Gholami et al. [95] succeeded in synthesizing silk fibroin nanoparticles of up to 80 nm on average. The authors showed that lower concentrations, lower feed rates, and longer distances between the needle and the collector led to a decrease in mean particle size. Increasing the voltage to 20 kV decreased the size of the particles but voltages higher than this produced an increase in the particle size.

4.2.4 Microfluidics

Microfluidic equipment can also be used for the preparation of nanoparticles. Microfluidic kits are devices, generally the size of millimeters/centimeters, that contain microcapillaries specially designed for mixing fluids [96, 97]. A representative image of these is shown in **Figure 6**. These types of equipment allow precise manipulation of liquids (like the dissolution of silk and the antisolvent) by means of the control of the parameters of the process such as the total flow, the relations of speed between different lines of injection, etc. The greatest advantages provided by this equipment are the possibility of producing particles in continuous flow and with a narrow size distribution.

Wongpinyochit et al. [63] have used a commercial microfluidic kit to mix a 3% wt solution of silk fibroin with acetone or isopropanol as an antisolvent. Through the use of different mixing conditions, the authors were able to control the final size of the nanoparticles obtained, which varied between 110 and 310 nm, with polydispersity and Z-potential indices between 0.1/0.25 and $-20/-30$ mV, respectively.

4.2.5 Salting-out

Phase separation has also been used for the preparation of nanoparticles using the salting-out method. For example, by adding potassium phosphate to a solution of silk fibroin, Lammel et al. [98] prepared fibroin particles with sizes varying between 500 and 2000 nm depending on the initial concentration of fibroin in solution. The authors revealed that, for the formation of nanoparticles, a salt concentration greater than 750 mM is required, otherwise, the solution gels.

5. Mechanism of nanoparticle formation in antisolvation processes

After having explained some of the synthesis methods, it is appropriate to mention the mechanism by which antisolvation can generate nano-sized particles. Upon

mixing the fibroin solution and the antisolvent, supersaturation occurs, leading to phase separation (precipitation). The mechanism can be divided into two steps, with a nucleation stage driven by supersaturation occurring first and then a growth stage. Growth can occur by two coagulation mechanisms: i) the nuclei of particles converge to form a larger particle or condensation and ii) the polymer units add to growing nuclei. This is exemplified in **Figure 7**. Condensation decreases supersaturation by reducing the mass of solute in the mixture and therefore competes with nucleation. Coagulation can reduce the rate of condensation by reducing the total number of particles and therefore the surface area [99]. Supersaturation influences nucleation and growth rates to different degrees. The nucleation rate depends more strongly on supersaturation than the condensation rate. High nucleation rates offer the potential to produce a large number of submicron particles in the final suspension if growth can be controlled. This process can be compared with the formation of crystals in the order of millimeters for X-ray crystallography when it is sought to obtain a low number of nuclei and greater growth in slow nucleation processes.

The key to generate rapid nucleation is to achieve rapid supersaturation. This process will be directly influenced by mixing and phase separation, which can be represented by the Damkohler number (Da) defined as the relationship between the mixing time (τ_{mix}) and the total precipitation time (τ):

$$Da = \frac{\tau_{mix}}{\tau} \quad (1)$$

Under poor mixing conditions, τ_{mix} is large (as is Da) and the nucleation rate is slow relative to the growth rate, resulting in large particles and wide size distributions. As the τ_{mix} is reduced with respect to the τ , greater supersaturation and faster nucleation are achieved, resulting in smaller particles with narrow size distribution [87].

The τ_{mix} can be reduced by reducing the size of the droplets (increasing the surface/volume ratio) of fibroin solution that meet the antisolvent, favoring mass transfer. Reduction in droplet size is typically achieved by increasing Reynolds number which produces turbulent flow and thus results in dissolution jet

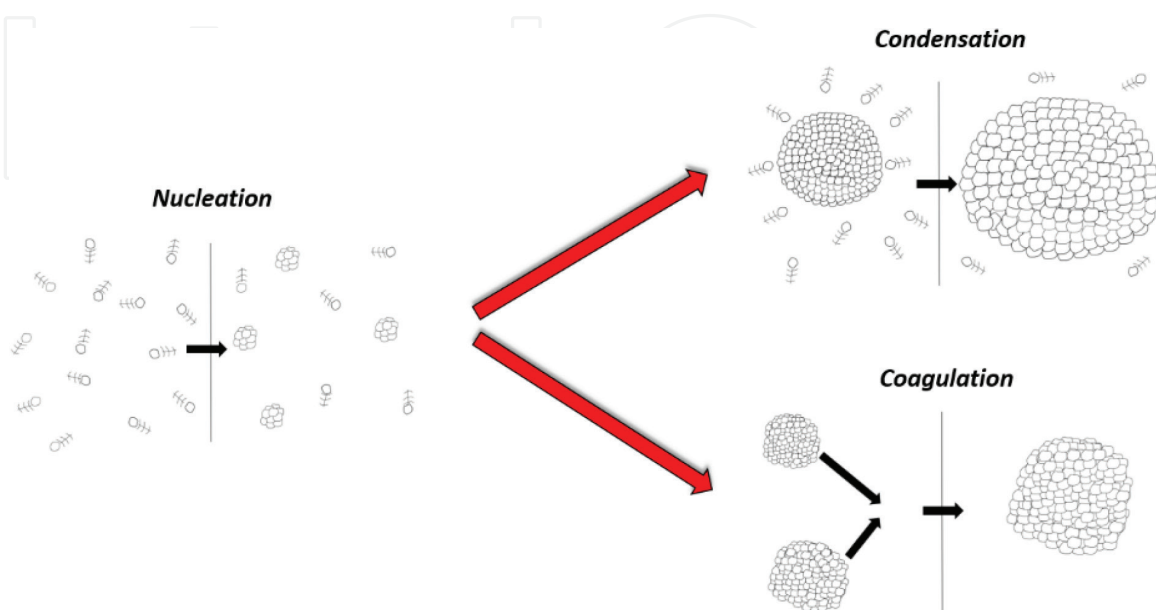


Figure 7. Scheme representing the mechanism of precipitation by nucleation and growth of particles by coagulation and condensation.

fragmentation. In fact, this is the goal of previously proposed methods such as the coaxial injector [45, 88], SEDS [90], electrospray [95] and microfluidic equipment [63].

According to Eq. (1), another strategy to reduce Da is to increase the τ . This can be achieved by adding stabilizers that interact with the polymer units generating steric hindrances that retard growth by condensation and coagulation [87]. According to Matteucci et al. [87], adding the stabilizers to the antisolvent is more effective in preventing the growth of the particles than adding them to the polymer solution. This is because, when placed in the antisolvent, the stabilizing agents are more available to interact with the polymeric units, as they do not need to diffuse across the interface from the overall aqueous phase to the organic phase.

Temperature is another important thermodynamic control factor for the preparation of nanoparticles by antisolvation that affects the formation of particles in different ways. Firstly, an increase in temperature leads to an increase in the solubility of the polymer and therefore reduces the degree of supersaturation when mixing the solutions, favoring slow nucleation. Secondly, elevated temperatures increase diffusion and growth kinetics at the interface of the particle boundary layer. And thirdly, higher solubility also increases Oswald's maturation rate [100]. For these reasons, a reduced temperature in the precipitation stage is preferable for the formation of small nanoparticles.

6. Nanoparticle drug loading

The loading of drugs can be carried out mainly by two approaches, (i) during the nanoparticle formation process or (ii) a posteriori, by adsorption of the drug on the surface of the nanoparticle. The first approach can be achieved by adding the drug to the polymer solution (nanoparticle matrix) [88] or the antisolvent [101] before mixing both. This approach is often referred to as coprecipitation because the polymer and drug precipitate together. In contrast to this method, adsorption of the drug to the surface of the nanoparticle can be achieved by incubating the nanoparticles in a solution of the drug. These methods have advantages and disadvantages. On the one hand, the first method is usually simpler, since the loading and preparation of the nanoparticle are carried out in a single step. However, this process could affect the formation of the nanoparticle and therefore the second method could be preferential. On the other hand, drug release profiles must be considered. As demonstrated by Montalbán et al. [88], particles charged by coprecipitation have slower release profiles compared to particles charged by absorption. This is to be expected since, in the latter, the drug is on the surface of the nanoparticle and readily available to the medium.

Drug loading and encapsulation efficiency depend on drug-polymer interactions and the presence of functional groups (i.e, hydroxyl, carboxyl, etc.) in both. Montalbán et al. [102] used computational methods such as blind docking and molecular dynamics simulations to study the interactions of different drugs with silk fibroin nanoparticles. The authors found a strong correlation between drug-fibroin interactions and their loading content. Similarly, drugs with weaker interactions had a higher release rate and a higher percentage of loaded drug release.

7. Conclusions

Silk fibroin of the *Bombyx mori* silkworm is a natural, protein polymer that presents an interesting combination of mechanical properties, such as flexibility

and resistance which are still difficult to achieve with synthetic polymers. Furthermore, fibroin is biodegradable and biocompatible, which makes it an excellent material for the production of nanoparticles for drug delivery.

Although the remarkable mechanical resistance of fibroin is one of the attractive properties of the biomaterial, the nanoparticle synthesis process is hampered by its high stability, due to the high number of hydrogen bonds in its secondary structure, mostly in the form of antiparallel β -sheets. A recent method, developed by our research group, is based on the use of ionic liquids to dissolve native fibroin and has allowed the production of nanoparticles in an easy and scalable process for industry.

The silk fibroin nanoparticle synthesis process comprises several stages. Firstly, the fibroin is purified by removing the sericin (a method known as degumming). Secondly, fibroin must be dissolved in its monomeric units and, subsequently, regenerated into nanoparticles. Each of these steps can have significant effects on the secondary structure of the protein and given the implications that it has on the resistance, degradability and biocompatibility of the final product, their study is essential.

Acknowledgements


This publication is part of the grant ref. CTQ2017-87708-R funded by MCIN/AEI/ 10.13039/501100011033 and by “ERDF A way of making Europe” and grant ref. PID2020-113081RB-I00 funded by MCIN/AEI/ 10.13039/501100011033. In addition, the publication is also part of the grant ref. 20977/PI/18 funded by the research support program of the Seneca Foundation of Science and Technology of Murcia, Spain. Marta G. Fuster acknowledges support from FPI grant (Ref. PRE2018-086441) funded by MCIN/AEI/ 10.13039/501100011033 and by “ESF Investing in your future”. Mercedes G. Montalbán acknowledges support from the University of Murcia and Santander Bank through the research project (Ref. RG2020-002UM) associated with her postdoctoral contract.

Author details

Guzmán Carissimi, Mercedes G. Montalbán*, Marta G. Fuster and Gloria Villora
Faculty of Chemistry, Chemical Engineering Department, Regional Campus
of International Excellence “Campus Mare Nostrum”, University of Murcia,
Murcia, Spain

*Address all correspondence to: mercedes.garcia@um.es

IntechOpen

© 2021 The Author(s). Licensee IntechOpen. This chapter is distributed under the terms of the Creative Commons Attribution License (<http://creativecommons.org/licenses/by/3.0>), which permits unrestricted use, distribution, and reproduction in any medium, provided the original work is properly cited. 

References

- [1] Good IL, Kenoyer JM, Meadow RH. New evidence for early silk in the Indus civilization. *Archaeometry*. 2009;51(3):457-466.
- [2] Vepari C, Kaplan DL, Charu Vepari; David L. Kaplan. Silk as a Biomaterial. *Prog Polym Sci*. 2009;32(8-9):991-1007.
- [3] Janani G, Kumar M, Chouhan D, Moses JC, Gangrade A, Bhattacharjee S, et al. Insight into Silk-Based Biomaterials: From Physicochemical Attributes to Recent Biomedical Applications. *ACS Appl Bio Mater*. 2019;2(12):5460-5491.
- [4] Aramwit P. Biomaterials for Wound-Healing Applications Complimentary Contributor Copy. 2015;(January):49-104.
- [5] Altman GH, Diaz F, Jakuba C, Calabro T, Horan RL, Chen J, et al. Silk-based biomaterials. *Biomaterials*. 2003;24(3):401-416.
- [6] Pérez-Rigueiro J, Viney C, Llorca J, Elices M. Mechanical properties of single-brin silkworm silk. *J Appl Polym Sci*. 2000;75(10):1270-1277.
- [7] Cunniff PM, Fossey SA, Auerbach MA, Song JW, Kaplan DL, Adams WW, et al. Mechanical and thermal properties of dragline silk from the spider *Nephila clavipes*. *Polym Adv Technol*. 1994 Aug;5(8):401-410.
- [8] Pins GD, Christiansen DL, Patel R, Silver FH. Self-assembly of collagen fibers. Influence of fibrillar alignment and decorin on mechanical properties. *Biophys J*. 1997;73(4):2164-2172.
- [9] Engelberg I, Kohn J. Physico-mechanical properties of degradable polymers used in medical applications: A comparative study. *Biomaterials*. 1991 Apr;12(3):292-304.
- [10] Gosline JM, Guerette PA, Ortlepp CS, Savage KN. The mechanical design of spider silks: From fibroin sequence to mechanical function. *J Exp Biol*. 1999;202(23):3295-3303.
- [11] Tesoro G. Textbook of polymer science, 3rd ed., Fred W. Billmeyer, Jr., Wiley-Interscience, New York, 1984, 578 pp. No price given. *J Polym Sci Polym Lett Ed*. 1984 Dec;22(12):674-674.
- [12] Wang W, Huang M-H, Dong X-L, Chai C-L, Pan C-X, Tang H, et al. Combined Effect of Cameo2 and CBP on the Cellular Uptake of Lutein in the Silkworm, *Bombyx mori*. *PLoS One*. 2014;9(1):e86594.
- [13] Sehnal F, Sutherland T. Silks produced by insect labial glands. *Prion*. 2008;2(4):145-153.
- [14] Asakura T, Ashida J, Yamane T, Kameda T, Nakazawa Y, Ohgo K, et al. A repeated β -turn structure in poly(Ala-Gly) as a model for silk I of *Bombyx mori* silk fibroin studied with two-dimensional spin-diffusion NMR under off magic angle spinning and rotational echo double resonance. *J Mol Biol*. 2001;306(2):291-305.
- [15] Kumar JP, Mandal BB. Antioxidant potential of mulberry and non-mulberry silk sericin and its implications in biomedicine. *Free Radic Biol Med*. 2017;108(February):803-818.
- [16] He YX, Zhang NN, Li WF, Jia N, Chen BY, Zhou K, et al. N-terminal domain of *Bombyx mori* fibroin mediates the assembly of silk in response to pH decrease. *J Mol Biol*. 2012;418(3-4):197-207.
- [17] Jin H-J, Kaplan DL. Mechanism of silk processing in insects and spiders. *Nature*. 2003 Aug;424(6952):1057-1061.
- [18] Asakura T, Yao J. ¹³C CP/MAS NMR study on structural heterogeneity in

Bombyx mori silk fiber and their generation by stretching. *Protein Sci.* 2002;11(11):2706-2713.

[19] Vollrath F, Knight DP. Liquid crystalline spinning of spider silk. *Nature.* 2001;410(6828):541-548.

[20] Hao LC, Sapuan SM, Hassan MR, Sheltami RM. Natural fiber reinforced vinyl polymer composites. *Natural Fibre Reinforced Vinyl Ester and Vinyl Polymer Composites.* Elsevier Ltd; 2018. 27-70 p.

[21] Aramwit P. Introduction to biomaterials for wound healing. In: *Wound Healing Biomaterials.* 2016, Woodhead Publishing; p. 3-38.

[22] Volkov V, Ferreira A V., Cavaco-Paulo A. On the Routines of Wild-Type Silk Fibroin Processing Toward Silk-Inspired Materials: A Review. *Macromol Mater Eng.* 2015;300(12): 1199-1216.

[23] Greving I, Cai M, Vollrath F, Schniepp HC. Shear-induced self-assembly of native silk proteins into fibrils studied by atomic force microscopy. *Biomacromolecules.* 2012;13(3):676-682.

[24] Padamwar MN, Pawar AP. Silk sericin and its application : A review. *J Sci Ind Res (India).* 2004;63(10): 323-329.

[25] Inoue S, Tanaka K, Arisaka F, Kimura S, Ohtomo K, Mizuno S. Silk fibroin of *bombyx mori* is secreted, assembling a high molecular mass elementary unit consisting of H-chain, L-chain, and P25, with a 6:6:1 molar ratio. *J Biol Chem.* 2000;275(51): 40517-40528.

[26] Guo C, Li C, Kaplan DL. Enzymatic Degradation of Bombyx mori Silk Materials: A Review. *Biomacromolecules.* 2020;21(5): 1678-1686.

[27] Lotz B, Colonna Cesari F. The chemical structure and the crystalline structures of *bombyx mori* silk fibroin. *Biochimie.* 1979;61(2):205-214.

[28] Carissimi G, Baronio CM, Montalbán MG, Vllora G, Barth A. On the Secondary Structure of Silk Fibroin Nanoparticles Obtained Using Ionic Liquids: An Infrared Spectroscopy Study. *Polymers (Basel).* 2020 Jun;12(6): 1294.

[29] Holland C, Numata K, Rnjak-Kovacina J, Seib FP. The Biomedical Use of Silk: Past, Present, Future. *Adv Healthc Mater.* 2019;8(1).

[30] Drummy LF, Farmer BL, Naik RR. Correlation of the β -sheet crystal size in silk fibers with the protein amino acid sequence. *Soft Matter.* 2007;3(7): 877-882.

[31] Martel A, Burghammer M, Davies RJ, Riekel C. Thermal Behavior of Bombyx mori Silk: Evolution of Crystalline Parameters, Molecular Structure, and Mechanical Properties. *Biomacromolecules.* 2007 Nov;8(11): 3548-3556.

[32] Pérez-Rigueiro J, Elices M, Plaza GR, Guinea G V. Similarities and Differences in the Supramolecular Organization of Silkworm and Spider Silk. *Macromolecules.* 2007 Jul;40(15): 5360-5365.

[33] Liang K, Gong Y, Fu J, Yan S, Tan Y, Du R, et al. Microstructural change of degummed Bombyx mori silk: An in situ stretching wide-angle X-ray-scattering study. *Int J Biol Macromol.* 2013 Jun;57:99-104.

[34] Wang X, Yucel T, Lu Q, Hu X, Kaplan DL. Silk nanospheres and microspheres from silk/pva blend films for drug delivery. *Biomaterials.* 2010; 31(6):1025-1035.

[35] Catto V, Farè S, Cattaneo I, Figliuzzi M, Alessandrino A, Freddi G,

et al. Small diameter electrospun silk fibroin vascular grafts: Mechanical properties, in vitro biodegradability, and in vivo biocompatibility. *Mater Sci Eng C*. 2015;54:101-111.

[36] Thurber AE, Omenetto FG, Kaplan DL. In vivo bioresponses to silk proteins. *Biomaterials*. 2015;71:145-157.

[37] Soong HK, Kenyon KR. Adverse Reactions to Virgin Silk Sutures in Cataract Surgery. *Ophthalmology*. 1984 May;91(5):479-483.

[38] Panilaitis B, Altman GH, Chen J, Jin HJ, Karageorgiou V, Kaplan DL. Macrophage responses to silk. *Biomaterials*. 2003;24(18):3079-3085.

[39] Carissimi G, Lozano-Pérez AA, Montalbán MG, Aznar-Cervantes SD, Cenis JL, Vllora G. Revealing the Influence of the Degumming Process in the Properties of Silk Fibroin Nanoparticles. *Polymers (Basel)*. 2019; 11(12).

[40] Meinel L, Hofmann S, Karageorgiou V, Kirker-Head C, McCool J, Gronowicz G, et al. The inflammatory responses to silk films in vitro and in vivo. *Biomaterials*. 2005 Jan;26(2):147-155.

[41] Santin M, Motta A, Freddi G, Cannas M. In vitro evaluation of the inflammatory potential of the silk fibroin. *J Biomed Mater Res*. 1999 Sep;46(3):382-389.

[42] Seo YK, Choi GM, Kwon SY, Lee HS, Park YS, Song KY, et al. The Biocompatibility of Silk Scaffold for Tissue Engineered Ligaments. *Key Eng Mater*. 2007 Jul;342-343:73-76.

[43] Tan M, Liu W, Liu F, Zhang W, Gao H, Cheng J, et al. Silk fibroin-coated nanoagents for acidic lysosome targeting by a functional preservation strategy in cancer chemotherapy. *Theranostics*. 2019;9(4):961-973.

[44] Totten JD, Wongpinyochit T, Carrola J, Duarte IF, Seib FP. PEGylation-Dependent Metabolic Rewiring of Macrophages with Silk Fibroin Nanoparticles. *ACS Appl Mater Interfaces*. 2019;11(16):14515-14525.

[45] Fuster MG, Carissimi G, Montalbán MG, Vllora G. Improving Anticancer Therapy with Naringenin-Loaded Silk Fibroin Nanoparticles. *Nanomater (Basel)*. 2020;10(4).

[46] Lozano-Pérez AA, Rodríguez-Nogales A, Ortiz-Cullera V, Algieri F, Garrido-Mesa J, Zorrilla P, et al. Silk fibroin nanoparticles constitute a vector for controlled release of resveratrol in an experimental model of inflammatory bowel disease in rats. *Int J Nano medicine*. 2014;9:4507-4520.

[47] Giménez-Siurana A, García FG, Bernabeu AP, Lozano-Pérez AA, Aznar-Cervantes SD, Cenis JL, et al. Chemoprevention of experimental periodontitis in diabetic rats with silk fibroin nanoparticles loaded with resveratrol. *Antioxidants*. 2020;9(1):1-13.

[48] Rodríguez-Nogales A, Algieri F, De Matteis L, Lozano-Pérez AA, Garrido-Mesa J, Vezza T, et al. Intestinal anti-inflammatory effects of RGD-functionalized silk fibroin nanoparticles in trinitrobenzenesulfonic acid-induced experimental colitis in rats. *Int J Nanomedicine*. 2016;11:5945-5958.

[49] Horan RL, Antle K, Collette AL, Wang Y, Huang J, Moreau JE, et al. In vitro degradation of silk fibroin. *Biomaterials*. 2005;26(17):3385-3393.

[50] Brown J, Lu CL, Coburn J, Kaplan DL. Impact of silk biomaterial structure on proteolysis. *Acta Biomater*. 2015;11(1):212-221.

[51] Li M, Ogiso M, Minoura N. Enzymatic degradation behavior of

- porous silk fibroin sheets. *Biomaterials*. 2003;24(2):357-365.
- [52] Nair LS, Laurencin CT. Biodegradable polymers as biomaterials. *Prog Polym Sci*. 2007;32(8-9):762-798.
- [53] Cao Y, Wang B. Biodegradation of silk biomaterials. *Int J Mol Sci*. 2009; 10(4):1514-1524.
- [54] Wongpinyochit T, Johnston BF, Seib FP. Degradation Behavior of Silk Nanoparticles - Enzyme Responsiveness. *ACS Biomater Sci Eng*. 2018;4(3):942-951.
- [55] Wang L, Luo Z, Zhang Q, Guan Y, Cai J, You R, et al. Effect of Degumming Methods on the Degradation Behavior of Silk Fibroin Biomaterials. *Fibers Polym*. 2019;20(1):45-50.
- [56] Zuo B, Dai L, Wu Z. Analysis of structure and properties of biodegradable regenerated silk fibroin fibers. *J Mater Sci*. 2006;41(11): 3357-3361.
- [57] Wang Z, Yang H, Li W, Li C. Effect of silk degumming on the structure and properties of silk fibroin. *J Text Inst*. 2018;5000(May):1-7.
- [58] Bhardwaj N, Rajkhowa R, Wang X, Devi D. Milled non-mulberry silk fibroin microparticles as biomaterial for biomedical applications. *Int J Biol Macromol*. 2015;81:31-40.
- [59] Rajkhowa R, Wang L, Wang X. Ultra-fine silk powder preparation through rotary and ball milling. *Powder Technol*. 2008;185(1):87-95.
- [60] Kazemimostaghim M, Rajkhowa R, Tsuzuki T, Wang X. Production of submicron silk particles by milling. *Powder Technol*. 2013;241:230-235.
- [61] Rajkhowa R, Wang L, Kanwar J, Wang X. Fabrication of ultrafine powder from eri silk through attritor and jet milling. *Powder Technol*. 2009;191(1-2):155-163.
- [62] Jacobs M, Heijnen N, Bastiaansen C, Lemstra P. Production of fine powder from silk by radiation. *Macromol Mater Eng*. 2000;283:126-131.
- [63] Wongpinyochit T, Totten JD, Johnston BF, Seib FP. Microfluidic-assisted silk nanoparticle tuning. *Nanoscale Adv*. 2019;1(2):873-883.
- [64] Rockwood DN, Preda RC, Yücel T, Wang X, Lovett ML, Kaplan DL. Materials fabrication from Bombyx mori silk fibroin. *Nat Protoc*. 2011; 6(10):1612-1631.
- [65] Ajisawa A. Dissolution aqueous of silk fibroin with calciumchloride / ethanol solution. *J Sericultural Sci Japan*. 1997;67(2):91-94.
- [66] Zheng Z, Guo S, Liu Y, Wu J, Li G, Liu M, et al. Lithium-free processing of silk fibroin. *J Biomater Appl*. 2016;31(3): 450-463.
- [67] Shen T, Wang T, Cheng G, Huang L, Chen L, Wu D. Dissolution behavior of silk fibroin in a low concentration CaCl₂-methanol solvent: From morphology to nanostructure. *Int J Biol Macromol*. 2018;113:458-463.
- [68] Mathur AB, Tonelli A, Rathke T, Hudson S. The dissolution and characterization of bombyx mori silk fibroin in calcium nitrate-methanol solution and the regeneration of films. *Biopolym - Nucleic Acid Sci Sect*. 1997;42(1):61-74.
- [69] Ha SW, Park YH, Hudson SM. Dissolution of bombyx mori silk fibroin in the calcium nitrate tetrahydrate-methanol system and aspects of wet spinning of fibroin solution. *Biomacromolecules*. 2003;4(3):488-496.
- [70] Cheng G, Wang X, Tao S, Xia J, Xu S. Differences in regenerated silk

fibroin prepared with different solvent systems: From structures to conformational changes. *J Appl Polym Sci.* 2015 Jun;132(22):1-8.

[71] Ajisawa A. Dissolution of silk fibroin with calciumchloride/ethanol aqueous solution. *J Seric Sci Jpn.* 1997;67(2):91-94.

[72] Kanbak M, Karagoz AH, Erdem N, Oc B, Saricaoglu F, Ertas N, et al. Renal Safety and Extrahepatic Defluorination of Sevoflurane in Hepatic Transplantations. *Transplant Proc.* 2007;39(5):1544-1548.

[73] Phillips DM, Drummy LF, Conrady DG, Fox DM, Naik RR, Stone MO, et al. Dissolution and Regeneration of *Bombyx mori* Silk Fibroin Using Ionic Liquids. *J Am Chem Soc.* 2004;126(10):14350-14351.

[74] Hernández-Fernández FJ, de los Ríos AP, Tomás-Alonso F, Gómez D, Rubio M, Vllora G. Integrated reaction/separation processes for the kinetic resolution of rac-1-phenylethanol using supported liquid membranes based on ionic liquids. *Chem Eng Process Intensif.* 2007;46(9):818-824.

[75] Hernández-Fernández FJ, de los Ríos AP, Tomás-Alonso F, Gómez D, Vllora G. On the development of an integrated membrane process with ionic liquids for the kinetic resolution of rac-2-pentanol. *J Memb Sci.* 2008;314(1-2):238-246.

[76] Rogers RD, Seddon KR. Ionic Liquids - Solvents of the Future? Vol. 302, *Science.* 2003. p. 792-3.

[77] Lozano-Pérez AA, Montalbán MG, Aznar-Cervantes SD, Cragolini F, Cenis JL, Vllora G. Production of silk fibroin nanoparticles using ionic liquids and high-power ultrasounds. *J Appl Polym Sci.* 2014;132, 41702.

[78] Wang Q, Yang Y, Chen X, Shao Z. Investigation of Rheological Properties

and Conformation of Silk Fibroin in the Solution of AmimCl. *Biomacromolecules.* 2021;13(6):1875-1881.

[79] Zhang Y-Q, Shen W-D, Xiang R-L, Zhuge L-J, Gao W-J, Wang W-B. Formation of silk fibroin nanoparticles in water-miscible organic solvent and their characterization. *J Nanoparticle Res.* 2007;9(5):885-900.

[80] ZhuGe DL, Wang LF, Chen R, Li XZ, Huang ZW, Yao Q, et al. Cross-linked nanoparticles of silk fibroin with proanthocyanidins as a promising vehicle of indocyanine green for photo-thermal therapy of glioma. *Artif Cells, Nanomedicine Biotechnol.* 2019;47(1):4293-4304.

[81] Kundu J, Chung Y-I, Kim YH, Tae G, Kundu SC. Silk fibroin nanoparticles for cellular uptake and control release. *Int J Pharm.* 2010;388(1):242-250.

[82] Perteghella, Sottani, Coccè, Negri, Cavicchini, Alessandri, et al. Paclitaxel-Loaded Silk Fibroin Nanoparticles: Method Validation by UHPLC-MS/MS to Assess an Exogenous Approach to Load Cytotoxic Drugs. *Pharmaceutics.* 2019 Jun;11(6):285.

[83] Wongpinyochit T, Johnston BF, Philipp Seib F. Manufacture and drug delivery applications of silk nanoparticles. *J Vis Exp.* 2016;2016(116):1-9.

[84] Li H, Tian J, Wu A, Wang J, Ge C, Sun Z. Self-assembled silk fibroin nanoparticles loaded with binary drugs in the treatment of breast carcinoma. *Int J Nanomedicine.* 2016;11:4373-4380.

[85] Yu S, Yang W, Chen S, Chen M, Liu Y, Shao Z, et al. Floxuridine-loaded silk fibroin nanospheres. *RSC Adv.* 2014;4(35):18171-18177.

[86] Wu P, Liu Q, Li R, Wang J, Zhen X, Yue G, et al. Facile preparation of paclitaxel loaded silk fibroin

- nanoparticles for enhanced antitumor efficacy by locoregional drug delivery. *ACS Appl Mater Interfaces*. 2013;5(23):12638-12645.
- [87] Matteucci ME, Hotze MA, Johnston KP, Williams RO. Drug nanoparticles by antisolvent precipitation: Mixing energy versus surfactant stabilization. *Langmuir*. 2006;22(21):8951-8959.
- [88] Montalbán M, Coburn J, Lozano-Pérez A, Cenis J, Villora G, Kaplan D. Production of Curcumin-Loaded Silk Fibroin Nanoparticles for Cancer Therapy. *Nanomaterials*. 2018;8(2):126.
- [89] Kiran E, Debenedetti PG, Peters CJ. *Supercritical Fluids*. 2000, Springer.
- [90] Xie M, Fan D, Li Y, He X, Chen X, Chen Y, et al. Supercritical carbon dioxide-developed silk fibroin nanopatform for smart colon cancer therapy. *Int J Nanomedicine*. 2017;12:7751-7761.
- [91] Zhao Z, Chen A, Li Y, Hu J, Liu X, Li J, et al. Fabrication of silk fibroin nanoparticles for controlled drug delivery. *J Nanoparticle Res*. 2012;14(4).
- [92] Chen BQ, Kankala RK, He GY, Yang DY, Li GP, Wang P, et al. Supercritical Fluid-Assisted Fabrication of Indocyanine Green-Encapsulated Silk Fibroin Nanoparticles for Dual-Triggered Cancer Therapy. *ACS Biomater Sci Eng*. 2018;4(10):3487-3497.
- [93] Reverchon E, De Marco I, Torino E. Nanoparticles production by supercritical antisolvent precipitation: A general interpretation. *J Supercrit Fluids*. 2007;43(1):126-138.
- [94] Jaworek A, Krupa A. Jet and drops formation in electrohydrodynamic spraying of liquids. A systematic approach. *Exp Fluids*. 1999;27(1):43-52.
- [95] Gholami A, Tavanai H, Moradi AR. Production of fibroin nanopowder through electrospraying. *J Nanoparticle Res*. 2011;13(5):2089-2098.
- [96] Composition P, Droplets V, Shishulin A V, Fedoseev VB. *Microfluidics-a review*. 1993;D.
- [97] Suh YK, Kang S. A review on mixing in microfluidics. *Micromachines*. 2010;1(3):82-111.
- [98] Lammel AS, Hu X, Park SH, Kaplan DL, Scheibel TR. Controlling silk fibroin particle features for drug delivery. *Biomaterials*. 2010;31(16):4583-4591.
- [99] Weber M, Thies M. Understanding the RESS Process. In: *Supercritical Fluid Technology in Materials Science and Engineering*. CRC Press; 2002.
- [100] Ostwald ripening. In: *IUPAC Compendium of Chemical Terminology*. Research Triagle Park, NC: IUPAC; 2007. p. 1824.
- [101] Perteghella S, Crivelli B, Catenacci L, Sorrenti M, Bruni G, Necchi V, et al. Stem cell-extracellular vesicles as drug delivery systems: New frontiers for silk/curcumin nanoparticles. *Int J Pharm*. 2017;520(1-2):86-97.
- [102] Montalbán MG, Chakraborty S, Peña-García J, Verli H, Villora G, Pérez-Sánchez H, et al. Molecular insight into silk fibroin based delivery vehicle for amphiphilic drugs: Synthesis, characterization and molecular dynamics studies. *J Mol Liq*. 2020;299:112156.